

A neutral hydrogen survey of polar ring galaxies

IV. Parkes observations

W. van Driel¹, F. Combes², M. Arnaboldi³, and L.S. Sparke⁴

¹ GEPI, Observatoire de Paris, Section de Meudon, 5 place Jules Janssen, F-92195 Meudon, France
e-mail: wim.vandriel@obspm.fr

² LERMA, Observatoire de Paris, 61 avenue de l'Observatoire, F-75014 Paris, France
e-mail: francoise.combes@obspm.fr

³ Osservatorio Astronomico di Capodimonte, V. Moiarriello 16, Napoli 80131, Italy
e-mail: magda@cerere.na.astro.it

⁴ Astronomy Department, University of Wisconsin-Madison, 475 N. Charter St., Madison WI 53706, U.S.A.
e-mail: sparke@uwast.astro.wisc.edu

Received 12/12/2001 ; accepted 12/2/2002

Abstract. A total of 33 polar ring galaxies and polar ring galaxy candidates were observed in the 21-cm H I line with the 64-m Parkes radio telescope. The objects, selected by their optical morphology, are all south of declination -39° and in only 5 of them H I had been reported previously. H I line emission was detected towards 18 objects, though in 3 cases the detection may be confused by another galaxy in the telescope beam, and one is a marginal detection. Eight objects were detected for the first time in H I, of which 5 did not have previously known redshifts.

Key words. *Galaxies: distances and redshifts Galaxies: general Galaxies: ISM Radio lines: galaxies*

1. Introduction

A polar-ring galaxy (hereafter referred to as PRG) consists of a flattened galaxy with an outer ring of gas, dust, and stars rotating in a plane approximately perpendicular to the central disc. Kinematically confirmed PRGs with a disc-dominated central galaxy tend to have wide, extended polar rings, while bulge-dominated objects show only short, narrow rings (Whitmore 1991; Reshetnikov & Sotnikova 1997). The PRGs probably represent merger products, and their study may give us valuable clues about the process and frequency of merging; their visible environment appears to be similar to that of normal galaxies (Brocca et al. 1997), which may support long formation and evolution times of the rings. In addition, measurement of rotation in the two nearly perpendicular planes of the ring and galaxy provide one of the few available probes of the three-dimensional shape of galactic gravitational potentials, and hence the shape of dark and luminous matter distributions.

The catalogue of Whitmore et al. (1990, hereafter PRC) provides us with over a hundred known polar-ring galaxies and PRG candidates, as well as a list of possibly related systems, divided into the four main categories

listed below. The updated number of objects per category listed here is different from that tabulated originally in the PRC, as since its publication the following 4 category B and 4 category C objects have been promoted to category A: B-03 (=IC 1689), B-17 (=UGC 9562), B-19 (=AM 2020-504), B-21 (=ESO603-G21), C-13 (=NGC 660), C-24 (=UGC 4261), C-27 (=UGC 4385) and C-45 (=NGC 5128); see references in Paper III. All of these will be considered members of the A category in our studies – note that of these objects only B-19 was observed in our present Parkes survey.

1. A: Kinematically-determined Polar-Ring Galaxies (17 objects)
2. B: Good Candidates for Polar-Ring Galaxies (20 objects)
3. C: Possible Candidates for Polar-Ring Galaxies (69 objects)
4. D: Systems Possibly Related to Polar-Ring Galaxies (51 objects)

The scientific goals of our 21-cm H I line surveys of PRGs are to:

1. Establish redshifts for the objects with previously unknown redshift.

2. Measure the amount of neutral hydrogen in these systems and examine its correlations with other observational parameters.
3. Identify objects for subsequent synthesis mapping; HI maps together with optical line studies will show which of the new morphological candidates are true polar-ring galaxies, and high-resolution maps will allow dynamical modelling.

Detailed observations of PRGs in the 21-cm HI line with large radio synthesis telescopes like the Australia Telescope, VLA or Westerbork, are crucial for an understanding of the dynamical state of these systems. Such mapping measures the distribution and the velocity field of gas in the rings, both of which are required for accurate determination of the shape of the dark halo. Together with optical absorption-line studies of the central galaxy, rotation in the ring gas determines whether morphological candidates are true polar rings. Further, knowledge of the ring mass is necessary to assess the stability of the rings against differential precession, an important consideration in estimating the time since its formation.

After having observed a sample of 47 PRC objects in the 21-cm HI line with the 140-foot (43-m) Green Bank telescope (Paper I), 44 PRC objects with the 100-m Effelsberg telescope (Huchtmeier 1996, Paper II) and 50 PRC objects with the 100-m class Nançay telescope (van Driel et al. 2000, Paper III), we now present observations of 33 PRC objects in the southern hemisphere with the 64-m Parkes telescope. Provisional results of a pilot PRG HI survey made at Parkes in 1992 by a member of our team, O.-G. Richter (private communication), were referred to in Paper III.

In Section 2 of the present paper the sample of PRGs observed in HI at Parkes is presented. The observations are described in Section 3, a brief discussion of the results is given in Section 4 and the conclusions are summarized in Section 5. An analysis of these, and all other available HI data on PRGs and related objects will be presented in paper V in these series (van Driel et al., in preparation).

2. The Parkes polar-ring galaxy sample

Listed in Table 1 are basic data for all 33 galaxies observed for our PRG HI survey at Parkes. These data, compiled from many sources, by no means form a homogeneous set. The sources used, in order of preference, are the online Lyon-Meudon Extragalactic Database (LEDA) [<http://leda.univ-lyon1.fr>], the NASA/IPAC Extragalactic Database (NED) [<http://nedwww.ipac.caltech.edu>] and the PRC. Generally, the data listed are mean, corrected values from the LEDA database, while the data in parentheses are uncorrected published values compiled in NED. Note that all radial velocities listed in this paper are heliocentric and calculated according to the conventional optical definition ($V=c(\lambda-\lambda_0)/\lambda_0$). The total blue magnitudes, B_T are sometimes indicative only, as they cannot be

assumed to be on the same photometric scale, nor do all represent the true total apparent blue magnitude as defined in, e.g., the RC3; sometimes a magnitude measured within a single aperture is used instead. Neither do the isophotal diameters, D_{25} , represent a homogeneous set of measurements, as they sometimes refer to the size of the faint polar ring, and sometimes to the size of the brighter equatorial disc.

Of the 33 PRC objects observed at Parkes, 28 were selected using the following criteria: (1) South of declination -39° (the limit of our Nançay survey; our Green Bank survey reached -45°), (2) from PRC Categories A, B or C, and (3) no published HI detection and not detected in the Parkes HIPASS Public Data Release spectra [<http://www.atnf.csiro.au/research/multibeam/release/>]. Of these 28, 14 have optical redshifts, 5 of which (of B-25, B-26, B-27, C-65 and C-72) are outside the range of the HIPASS spectra, -1281 to $12,741$ km s^{-1} .

Besides the 28 objects thus selected, the telescope time allocation also permitted us to observe the following 6 objects: three (PRC A-05 = NGC 4650A, C-11 = NGC 625 and C-42 = NGC 4672) that were detected in HIPASS and previously reported as detected in the literature, two (C-15 = ESO 199-IG12 and C-55 = ESO 143-G37) that were detected in HIPAS, and one (C-14 = NGC 979) whose previously reported detection seems due to radio interference. For details on the available HI data for all objects we refer to Table 2 and Section 4.1.

3. Observations

The observations with the Parkes 64-m telescope were made in August 2001, using about 75 hours of telescope time. The data were obtained with the 13-element 21-cm Multibeam receiver (Staveley-Smith et al. 1996), of which the inner 7 elements only were consecutively pointed towards the target galaxy. The FWHM of the telescope in the observing mode used at 21-cm wavelength is $14''.4$. The autocorrelator was divided into two pairs of cross-polarized receiver banks, each with 2048 channels and a 64 MHz bandpass, giving a radial velocity coverage of about $12,500$ km s^{-1} and a channel separation of 6.6 km s^{-1} . For objects with known redshifts, the centre frequencies of the two banks were generally tuned to an HI velocity of $5,500$ km s^{-1} or $15,000$ km s^{-1} , depending on the redshift. For the 3 objects (PRC B-18, C-22 and C-48) with redshifts in the overlapping region, $9,000$ to $12,000$ km s^{-1} , a centre velocity of $10,000$ km s^{-1} was used. For objects of unknown redshift, line searches were first made in the -1000 to $12,000$ km s^{-1} range and, if not detected, in the $8,500$ - $21,500$ km s^{-1} range; the two rms. noise levels listed in Table 1 for undetected objects refer to these two velocity search ranges. The observing time was distributed as equally as possible between the different line searches, about 1.25 hours per velocity range per object, hence the similarity in rms noise levels.

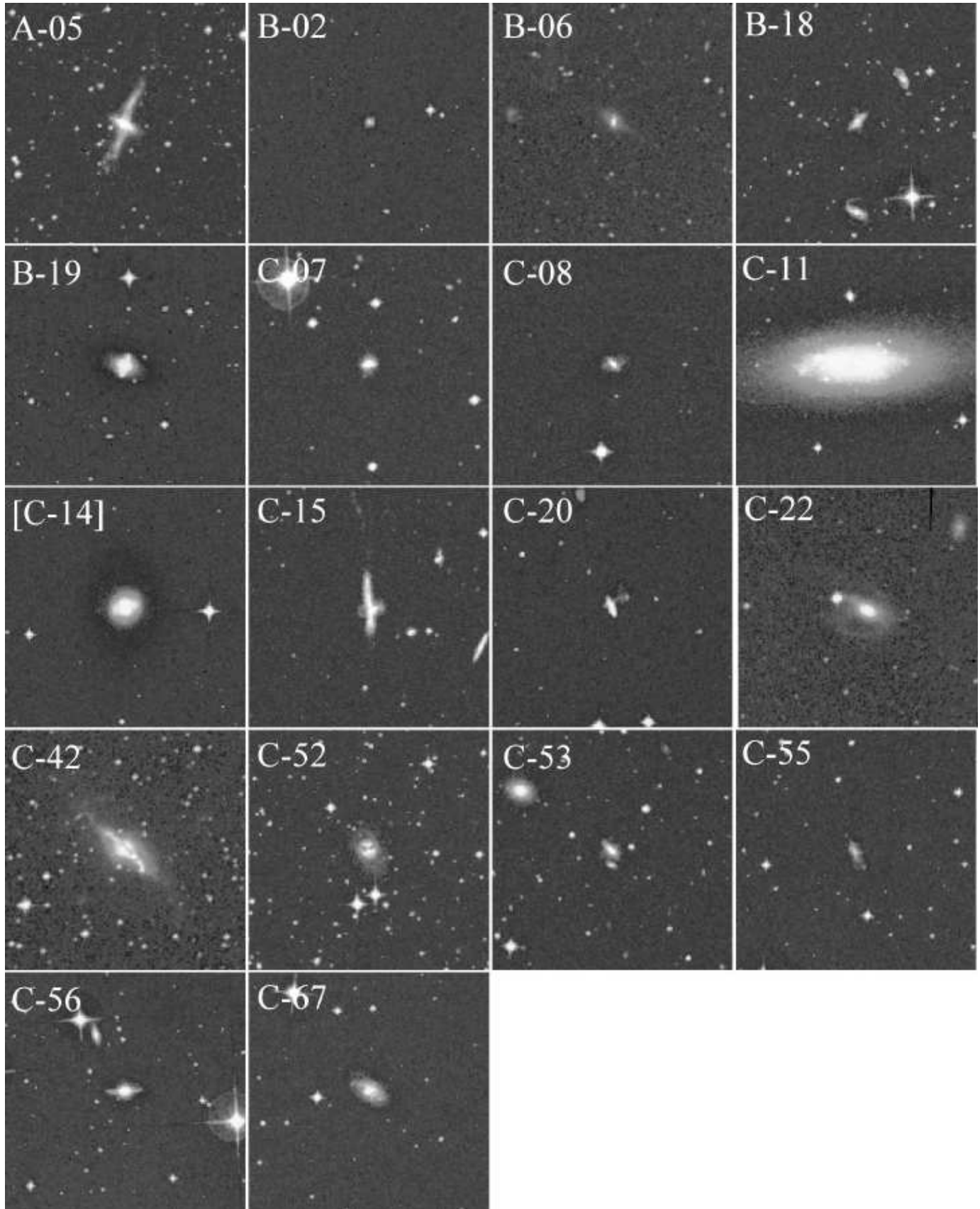


Fig. 1. Optical Digital Sky Survey images of all 18 PRC objects towards which H I line emission was detected at Parkes. Each galaxy is identified by its PRC name. Each image has a size of $5' \times 5'$. For comparison: the telescope's FWHM is $14''.4$.

Table 1. Basic data for the Parkes polar ring galaxy H I survey sample.

PRC	Ident.	RA	Dec	V_{opt}	B_T	D_{25}	V_{HI}	W_{50}	W_{20}	I_{HI}	rms	D	L_B [log] $L_{\odot,B}$	M_{HI} [log] M_{\odot}	M_{HI}/L_B $M_{\odot}/L_{\odot,B}$
		(J2000.0)		km/s	mag	'	km/s	km/s	km/s	Jy km/s	mJy	Mpc			
Kinematically-determined polar-ring galaxies															
A-05	NGC 4650A	12 44 48.8	-40 42 50	2808±97	13.91	1.5	2880±3	221	240	19.5	7.3	35.9	9.74	9.77	1.1
B-19	AM 2020-504	20 23 54.8	-50 39 05	4989±69	15.97	1.2	5006±43:	390	650:	6.1	4.4	65.5	9.44	9.44	2.2
Good candidates for polar-ring galaxies															
B-02	PGC 419347	01 15 28.7	-54 26 53		16.83	0.4	5361±27	98	225:	1.7	3.3	70.0	9.15	<i>confused?</i>	
B-04	PGC 145741	03 37 57.6	-48 55 40		(16.61)	0.6				<3.6	4.5/3.6				<2.4
B-05	PGC 415379	03 52 49.2	-54 49 50		16.46	0.5				<4.1	4.4/4.7				<2.4
B-06	AM 0442-622	04 43 07.6	-62 19 42		16.32	0.6	7165±27	308	435	2.8	3.8	92.7	9.60	9.76	1.4
B-18	AM 1934-563	19 38 38.7	-56 27 30	11649±60	15.93	0.6	11282±24	193	308	4.1	3.3	153.8	10.19	<i>confused</i>	
B-22	PGC 13177	23 31 54.6	-40 45 45		15.11	0.8				<3.9	4.5/4.2				<0.65
B-25	PGC 164989	23 51 41.3	-39 10 31	(19540±50)	16.08	0.6				<6.6	4.4	260.4	10.59	<11.0	<2.7
B-26	PGC 165022	23 53 20.1	-40 25 53	(16470)	(16.74)	0.7				<4.6	4.4	219.3	10.18	<10.7	<3.5
B-27	ESO 293-IG17	23 56 25.3	-39 10 36	15300±60	16.17	1.0				<5.4	4.5	203.8	10.34	<10.7	<2.4
Possible candidates for polar-ring galaxies															
C-07	ESO 113-IG4	01 00 34.2	-57 44 56	3130±200	15.67	0.6	3587±29	131	275:	2.1	4.3	46.2	9.25	9.03	0.6
C-08	ESO 243-IG19	01 02 49.2	-47 11 12		16.05	0.6	6438±40	335	435	3.2	5.1	84.9	9.63	9.73	1.3
C-10	ESO 152-IG3	01 28 24.8	-52 38 08	3450±60	16.17	0.4				<2.5	5.9	44.6	9.02	<9.1	<1.1
C-11	NGC 625	01 35 04.2	-41 26 15	391±44	11.61	6.3	396±1	79	112	32.1	9.9	4.6	8.87	8.20	0.2
C-14	NGC 979	02 31 38.7	-44 31 28		14.22	1.1	[5181	241		2.1	3.3]				<0.22
C-15	ESO 199-IG12	03 03 24.2	-50 29 51	7030±60	14.80	1.4	6873±18	409	532	10.0	5.6	89.8	10.18	10.28	1.3
C-16	AM 0320-495	03 21 56.0	-49 48 03		16.11	0.7				<4.0	3.8/5.1				<1.7
C-20	ESO 201-IG26	04 15 17.6	-50 56 43	3802±47	15.45	0.6	3745±6	213	225	4.1	5.2	47.7	9.37	9.35	0.95
C-21	PGC 495219	04 16 18.9	-47 49 14		16.88	0.6				<3.7	4.0/4.2				<3.2
C-22	ESO 202-G1	04 16 31.1	-47 50 51	10052±50	14.73	1.3	9780±30:	220	315:	1.4	3.1	128.2	10.52	<i>marginal</i>	
C-42	NGC 4672	12 46 15.4	-41 42 22	3346±63	14.10	2.2	3202±6	343	377	12.7	4.8	46.5	9.89	9.81	0.84
C-48	ESO 326-IG6	14 11 08.5	-40 06 22	8598±45	15.32	0.9				<5.3	5.1	111.3	10.16	<10.2	<1.1
C-52	ESO 232-G4	19 22 46.6	-51 00 08	5600:±200	14.81	1.3	4951±20	320	385	2.5	3.6	64.5	9.89	9.54	0.45
C-53	IC 4982	20 20 37.1	-71 01 45		15.58	0.6	6180±16	190	235	2.9	4.6	80.0	9.77	9.63	0.74
C-55	ESO 143-G37	20 37 48.0	-61 44 50		16.42	0.7	3265±9	90	151	4.8	5.1	42.2	8.87	9.31	2.7
C-56	PGC 128148	20 44 11.6	-61 59 19		15.75	0.8	3335±24	259	485	5.7	4.4	42.6	9.15	9.38	1.7
C-61	PGC 263886	21 20 56.6	-72 20 17		16.11	0.5				<4.4	4.3/5.5				<1.8
C-62	ESO 236-IG2	21 19 46.8	-52 14 16		16.35	0.5				<4.1	4.2/4.8				<2.1
C-65	ESO 287-IG50	21 41 57.9	-46 00 38	17700±35	15.76	0.6				<7.0	4.7	235.3	10.63	<11.0	<2.1
C-67	ESO 75-G55	22 06 24.9	-67 31 03		14.93	1.0	3541±10	173	193	3.3	3.0	45.2	9.53	9.20	0.47
C-68	PGC 127657	22 24 14.5	-66 02 18		14.73	0.9				<4.6	5.0/5.2				<0.54
C-72	ESO 240-IG16	23 44 48.1	-49 06 41	13664±60	15.88	0.6				<4.6	4.1	179.0	10.35	<10.5	<1.6

Notes: most optical data are mean, corrected values from the LEDA database; data in parentheses are literature values, from NED. For the estimated upper limits to the integrated H I line flux, I_{HI} , see Sect. 4. A ':' denotes an uncertain value. The line detected towards PRC C-14 seems due to nearby ESO 246-G22; for details on this object, and on the detections marked as 'confused' or 'marginal', see Sect. 4.1.

We calibrated, averaged and made a first baseline subtraction in our spectra using the standard multibeam receiver spectral line data reduction package available at the Parkes site, GRIDZILLA. The data were then reformatted, using a routine written by L.S. Staveley-Smith, for further reduction with the CLASS spectral line data reduction package. With CLASS we made a final, third-order polynomial baseline subtraction, and determined the global HI line parameters and rms. noise level in the spectra, after degrading the velocity resolution to 13.2 km s^{-1} for most spectra (see Sect. 4).

4. Results

The reduced Parkes 21-cm spectra are shown in Figure 1 for all objects towards which line emission was detected, clearly or tentatively. For discussion of possible confusion with other galaxies in the beam, see Section 4.1 – we assumed that the emission line detected toward PRC C-14 is due to a nearby galaxy. Basic optical and HI line parameters of all observed objects are listed in Table 1. For the optical data we preferentially used the mean parameters from the LEDA database, or literature values from NED if these were not available (for the optical redshift of PRC B-18, see Section 4.1).

Columns in Table 1 are as follows: (1) galaxy number in the PRC, (2) identifications in other catalogues, (3 & 4) optical centre position, which was used as pointing position for the HI observations, (5) optical systemic velocity and its estimated uncertainty, if available, (6) the total blue magnitude, uncorrected for Galactic or internal extinction, (7) blue major axis diameter at the 25 mag arcsec^{-2} isophotal level, (8) centre velocity of the HI profile and its estimated uncertainty (see below), (9) width of the HI profile measured at the 50% level of the peak flux density, (10) idem, at the 20% level, (11) integrated HI line flux or an estimated 3σ upper limit (see below), depending on the blue luminosity of the objects, if known (see text), (12) rms noise level of the spectrum; if two values are listed for an object, the first refers to the ~ 1000 to $12,000 \text{ km s}^{-1}$ velocity range and the second to the $\sim 8,500$ to $21,500 \text{ km s}^{-1}$ range, (13) distance, derived preferably using heliocentric systemic HI line velocities, or otherwise optical velocities, corrected to the Local Standard of Rest following the prescription of Sandage & Tammann (1981, RSA):

$$V_{LSR} = V_{hel} - 79 \cos l \cos b + 296 \sin l \cos b - 36 \sin b \quad [km s^{-1}] \quad (1)$$

and assuming a Hubble constant $H_0 = 75 \text{ km s}^{-1} \text{ Mpc}^{-1}$, (14) blue luminosity, (15) HI mass, derived straight from the measured integrated HI line fluxes without any correction factors, such as for beam filling:

$$M_{HI} = 2.356 \cdot 10^5 D^2 I_{HI} [M_{\odot}] \quad (2)$$

(16) ratio of the total HI mass and blue luminosity.

The instrumental velocity resolution of the reduced data is 13.2 km s^{-1} , except for the narrow profile of C-11 (6.6 km s^{-1}) and for the faint detection seen towards

C-14 (26.4 km s^{-1}). We estimated the uncertainties, $\sigma_{V_{HI}}$, in the central HI velocities, V_{HI} , following Fouqué et al. (1990):

$$\sigma_{V_{HI}} = 4R^{0.5} P_W^{0.5} X^{-1} [km/s] \quad (3)$$

where R is the velocity resolution in km s^{-1} , $P_W = (W_{20} - W_{50})/2$ in km s^{-1} and X is the signal-to-noise ratio of a spectrum, which we defined as the ratio of the peak flux density and the rms noise. According to Fouqué et al., the uncertainty in the linewidths is $2\sigma_{V_{HI}}$ for W_{50} and $3\sigma_{V_{HI}}$ for W_{20} .

As the HI linewidths of detected PRC objects show an increase with luminosity (van Driel et al., in prep.), though with large scatter, the estimated upper limits to the integrated HI line flux, I_{HI} , are 3σ values for flat-topped profiles with an estimated W_{20} width depending on the blue luminosity of the galaxies, consistent with the upper limits listed in Paper III. For the 9 objects of unknown redshift, including C-14, a W_{20} linewidth of 300 km s^{-1} , was assumed, a typical value for the entire sample. For the objects not detected in the -1000 to $21,500 \text{ km s}^{-1}$ range, the average rms noise level over this entire range was used to estimate the upper limit. The resulting M_{HI} and M_{HI}/L_B upper limits for the objects without known redshift are obviously only significant if their redshift in fact lies within the velocity range searched.

4.1. Notes on individual objects

The data on possible companions that may confuse the Parkes spectra were compiled using the online NED and LEDA databases, searching in an area of $22'$ diameter (i.e., 1.5 times the telescope's FWHM) centered on the pointing positions of the telescope (see Table 1). The published HI data on our target PRC objects are summarized and compared to our present Parkes results in Table 2.

Kinematically-determined polar-ring galaxies

A-05 (= NGC 4650A): This is probably the best-studied of all polar ring galaxies, see, e.g., Arnaboldi et al. (1997). Detected in the present survey and in 4 others, including two interferometric mappings (see Table 2). The VLA and Australia Telescope HI imaging show that our single-dish spectrum is not confused by the two other relatively bright, but early-type galaxies in the Parkes beam, NGC 4650 ($V_{opt} = 2859 \text{ km s}^{-1}$) and NGC 4650B ($V_{opt} = 2515 \text{ km s}^{-1}$). These early-type galaxies are expected to be gas-poor

B-19 (= AM 2020-504): This is the best-studied case of a polar ring around an elliptical galaxy (Arnaboldi et al. 1993a); the other case in our sample is PRC C-42, see below. The polar ring shows a gentle warp and is probably stable, giving time to stars to form and grow old. It has a UV spectrum typical of a starburst galaxy (Arnaboldi et al. 1993b). The object was detected in the present survey, at $V_{HI} = 5006 \pm 43 \text{ km s}^{-1}$. Our profile does not seem to be confused by another object in the beam. The HI line

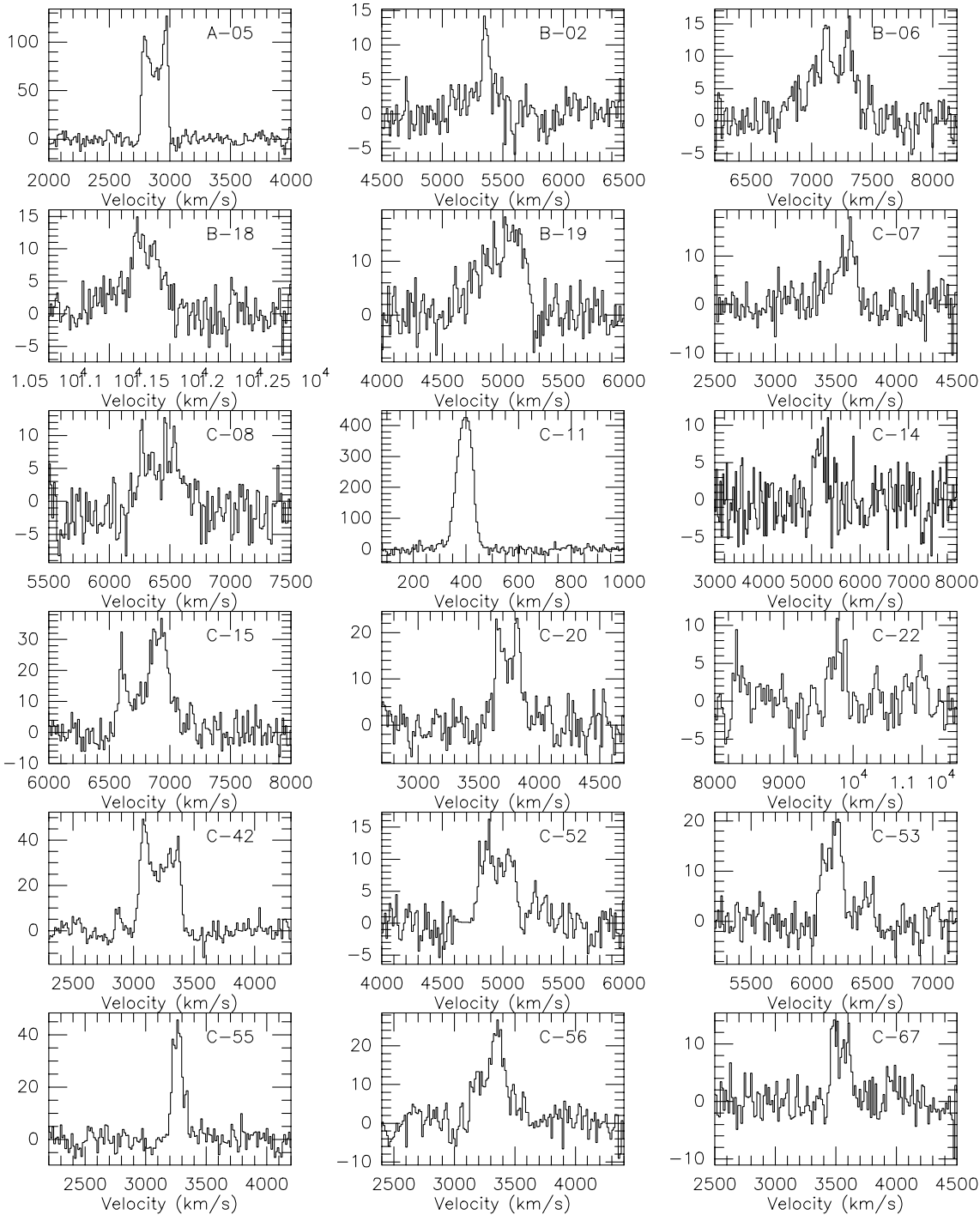


Fig. 2. Parkes 21-cm H I line spectra of all clear and marginal detections. Each galaxy is identified by its PRC number. The axes are heliocentric velocity in km s^{-1} , and flux density in mJy. The velocity resolution of the spectra is 13.2 km s^{-1} , except for C-11 (6.6 km s^{-1}) and C-14 (26.4 km s^{-1}).

velocity corresponds well to the mean optical value of the PRC object, $4989 \pm 69 \text{ km s}^{-1}$ (LEDA).

Just outside the telescope’s FWHM radius, two galaxies lie at about $8'$ distance from the PRC target: the quite face-on ($b/a=0.8$) 14.0 mag Sc type spiral ESO 234-G016 at $V_{\text{opt}}=5215 \pm 82 \text{ km s}^{-1}$ and the 14.6 mag Sbc type spiral

ESO 234-G017, of unknown redshift. Given the difference in optical velocities (225 km s^{-1}) and the range of velocities in our H I profile, it seems unlikely that the Parkes profile was confused by ESO 234-G016.

Good candidates

Table 2. Published H I data for the Parkes PRG sample.

PRC	Tel. code	V_{HI} km/s	I_{HI} Jy km/s	W_{50} km/s	W_{20} km/s	Ref.
A-05	P	2880	19.5	221	240	*
	P	2910			220	Ba97
	G43	2909	23.2	244		Ri94
	V	2910	16.0	231	243	vG87
	AT	2905	23.1	221	240	Ar97
C-11	P	396	32.1	79	112	*
	P	387	38.0		116	Re82
	P	387	26.0			Bo88
	G43	404	32.4			FT81
	G43	394	37.4	113		Ri94
	IAR	370	35.1	80	103	BM85
	V	406	30.6			Co00
C-14	P	[5141	2.1	241	241]	*
	P		<10.4			Ha81
C-42	G43	4775	26.2	678:		Ri94
	P	3202	12.7	343	377	*
	P	3289	15.6	356	403	Aa89
	G43	3242	7.7	401		Ri94

Telescope codes:

AT	Australia Telescope
G43	Green Bank 43-m
IAR	I.A.R. 30-m
P	Parkes 64-m
V	VLA

References:

Aa89	Aaronson et al. (1989)
Ar97	Arnaboldi et al. (1997)
BM85	Bajaja & Martin (1985)
Ba97	Barnes et al. (1997)
Bo88	Boissé et al. (1988)
Co00	Côté et al. (2000)
FT81	Fisher & Tully (1981)
Ha81	Hawarden et al. (1981)
Re82	Reif et al. (1982)
Ri94	Richter et al. (1994)
vG87	van Gorkom et al. (1987)
*	this paper

B-02 (= PGC 419347): This object does not have a known optical redshift. We detected an H I profile towards it, at $V_{HI}=5361\pm 27$ km s⁻¹. At 7.3 distance, around the telescope’s FWHM radius, lies 15.5 mag Sc? type spiral ESO 151-G37, with $V_{opt}=5452\pm 60$ km s⁻¹ (Mathewson & Ford 1996), 91 km s⁻¹ higher than the H I value. If the detection were in fact entirely due to ESO 151-G37, its integrated H I line flux would be ~ 3.4 Jy km s⁻¹, at $\sim 50\%$ beam efficiency, implying an M_{HI}/L_B ratio of 0.8 $M_\odot/L_{\odot,B}$. Such a ratio is about 2.5 times the average for Sc spirals (Roberts & Haynes 1994) and therefore highly unlikely. If, on the other hand, all H I were to be due to B-02 alone, its M_{HI}/L_B ratio would be 1.4 $M_\odot/L_{\odot,B}$, a quite common value for an object from PRC Category B. A long-slit H α spectrum of ESO 151-G37 (Mathewson & Ford 1996) shows a maximum rotational velocity, uncorrected for inclination, of 107 km s⁻¹, much larger than half the W_{50} width of our H I spectrum, 45 km s⁻¹. In conclusion, it is not very likely that our H I detection may be confused by nearby ESO 151-G37.

B-06 (= AM 0442-622): detected in the present survey, at $V_{HI}=7165$ km s⁻¹. The only other catalogued galaxy within the telescope’s FWHM, the low surface brightness object LSBG F118-043, of unknown redshift and B_T 18.7 mag. Though low surface brightness galaxies can be quite gas-rich, it is ~ 2.4 mag fainter than B-06 in the blue, and

hence not a likely candidate for confusion with our H I profile. The M_{HI}/L_B ratio of 1.4 $M_\odot/L_{\odot,B}$ derived for B-06 assuming that all detected gas resides in it is a quite common value among the PRC Category B objects.

B-18 (= AM 1934-563): detected in the present survey, at $V_{HI}=11282\pm 24$ km s⁻¹, with a W_{50} width of 193 km s⁻¹. Its nuclear H α and [NII] emission lines (Reshetnikov et al. 2001) indicate fast rotation of the gas in the innermost regions, reaching a projected rotational velocity of ~ 230 km s⁻¹ at $\sim 2''$ from the nucleus, as well as signs of Sy2 or LINER activity. Its mean optical systemic velocity listed in LEDA, 11703 ± 153 km s⁻¹, did not take into account the latter two of the four following published redshifts: 11556 ± 48 km s⁻¹ (Fisher et al. 1995), 11842 ± 120 km s⁻¹ (Allen et al. 1991), 11850 ± 200 km s⁻¹ (Fairall & Jones 1991) and 11613 ± 54 km s⁻¹ (Reshetnikov et al. 2001). From these three values, we derive a weighted mean value of $V_{opt}=11649\pm 60$ km s⁻¹, 367 km s⁻¹ ($\sim 6\sigma_{V_{opt}}$) lower than the H I value, a significantly large difference. Three galaxies of similar size and magnitude can be seen in Figure 1, which appear to form a triplet. Besides the PRC object, these are PGC 399718 ($B_T=15.7$ and $D_{25}=0'.7$) and PGC 400092 ($B_T=16.2$ and $D_{25}=0'.5$), both of unknown redshift. The M_{HI}/L_B ratio of 1.5 $M_\odot/L_{\odot,B}$ we would derive for B-18 if all H I were concentrated in it is quite common for a PRC Category B object, however. In conclusion, we cannot exclude that the H I profile may be confused with, or due to, another member of the triplet.

B-27 (= ESO 293-IG17): not detected in the present survey. Our Green Bank H I survey (Paper I) did not cover the optical redshift of the object ($15,300$ km s⁻¹), which was published afterwards.

Possible PRG candidates

C-07 (= ESO 113-IG4): an H I line was detected in the present survey, at $V_{HI}=3587\pm 29$ km s⁻¹. The optical systemic velocity, 3130 km s⁻¹ (from Keel 1985), is 477 km s⁻¹ lower than the H I value. Though its uncertainty is listed as 35 km s⁻¹ in LEDA, a value of 200 km s⁻¹ was quoted in Keel’s paper - we adopted the latter uncertainty. Given the relatively large uncertainties involved, the H I and optical velocities may be consistent. No candidates for confusion with our H I spectrum were found within the search area.

C-08 (= ESO 243-IG19): detected in the present survey, at $V_{HI}=6438\pm 40$ km s⁻¹. No optical redshift is known of this object. No candidates for confusion with our H I spectrum were found within the search area.

C-11 (= NGC 625): detected in the present survey and in 6 others (see Table 2), with good agreement between the global H I line parameters measured at different telescopes and in different studies. The galaxy was mapped in H I at the VLA (Côté et al. 2000), where a peculiar gas distribution and kinematics was found. The H I is rotating around the optical major axis, rather than the minor axis, though its distribution is elongated along the major axis - contrary to the situation in polar rings.

Multiple velocity peaks occur at many places in the VLA data. Consequently no HI rotation curve could be derived. The ionized gas in the galaxy also follows complex orbits (Marlowe et al. 1997), which do not match the HI kinematics, however. Its is a rather red system $(B-R) = 0.89$, with a smooth morphology reminiscent of lenticular galaxies, and strong emission lines, like a blue compact dwarf (Skillman et al. 2002) According to Côté et al., the seriously disturbed nature of NGC 625 is due to a major merger event rather than a case of bad digestion of an accreted HI cloud.

C-14 (= NGC 979): No optical velocity is known of this object, and it does not appear to have been detected in HI. A detection with the Green Bank 43-m telescope was reported in Paper I, with a centre velocity of 4775 km s^{-1} , an exceptionally large width of $W_{20}=678 \text{ km s}^{-1}$ and a peak flux density of $\sim 30 \text{ mJy}$, while at Parkes no line signal was detected by Hawarden et al. (1981), with a published upper limit to the integrated HI line flux of $10.4 \text{ Jy km s}^{-1}$. As no trace of the signal seen at Green Bank can be found in our Parkes data, which have an rms noise level of 3.3 mJy , it must have been due to interference. Our Parkes spectrum shows a marginal HI detection at $V_{HI}=5240 \text{ km s}^{-1}$, which is likely to be associated with ESO 246 G-22, a 14.4 mag SBc spiral with an optical redshift of $5127\pm 60 \text{ km s}^{-1}$ (LEDA), 9'1 from the PRC object. We therefore consider PRC C-14 to be undetected in our survey, and the upper limit to its M_{HI}/L_B ratio of $0.22 M_{\odot}/L_{\odot,B}$ listed in Table 1 was estimated using a 300 km s^{-1} linewidth, like for all objects of unknown redshift.

C-15 (= ESO199-12): A strong HI line was detected in the present survey, with $V_{HI}=6873\pm 18 \text{ km s}^{-1}$ and $W_{50}=409 \text{ km s}^{-1}$. There appears to be a faint detection in the Parkes HIPASS survey data, at $\sim 7000 \text{ km s}^{-1}$, with a peak flux density of about 30 mJy , like in our spectrum. The large uncertainty in the optical velocity of the object, as listed in LEDA, $6727\pm 358 \text{ km s}^{-1}$, is due to one discrepant measurement: $6296\pm 300 \text{ km s}^{-1}$ (Kirhakos & Steiner 1990), compared to the 7033 ± 35 and $7026\pm 75: \text{ km s}^{-1}$ from, respectively, Da Costa et al. (1991) and Chincarini et al. (1984). Therefore, the optical redshift is rather $7030\pm 60 \text{ km s}^{-1}$, 157 km s^{-1} (i.e., $2.5\sigma_{V_{opt}}$) higher than the HI value. The only other galaxy of significant size ($D_{25}=1'2$) within the telescope's FWHM is IC 1877, an edge-on Sb:pec spiral of unknown redshift and $B_T 16.2$ mag. It does not seem likely that this 1.4 mag fainter object would cause serious confusion in the HI spectrum of the target object. The M_{HI}/L_B ratio of $1.25 M_{\odot}/L_{\odot,B}$ we would derive if all HI was concentrated in the PRC object is not uncommon for PRC category-C objects.

C-16 (= AM 0320-495): our Parkes spectrum only shows an off-beam detection of an unidentified galaxy, with $V_{HI}=1023 \text{ km s}^{-1}$, $W_{50}=207 \text{ km s}^{-1}$ and $I_{HI}=-2.1 \text{ Jy km s}^{-1}$. It appears to be a sidelobe-detection of $B_T 13.6$ mag, Scd spiral IC 1914, at $27'3$ distance from the target object. *Observations of IC 1914* at Parkes by Longmore et al. (1982) show $V_{HI}=1037 \text{ km s}^{-1}$, $W_{50}=206 \text{ km s}^{-1}$ and $I_{HI}=53.0 \text{ Jy km s}^{-1}$.

C-20 (= ESO 201-IG26): detected in the present survey, at $V_{HI}=3745\pm 6 \text{ km s}^{-1}$, corresponding well with the optical systemic velocity of 3802 ± 47 (LEDA). Also in, the less sensitive, Parkes HIPASS data a tentative detection is seen at the same velocity. No candidates for confusion with our HI spectrum were found within the search area: at $2'4$ distance, low surface brightness object LSBG F202-064, of unknown redshift and $B_T 17.7$ mag, does not seem a likely candidate: though low surface brightness galaxies can be quite gas-rich, it is ~ 2.2 mag fainter than C-20. The M_{HI}/L_B ratio of $0.95 M_{\odot}/L_{\odot,B}$ derived for C-20 assuming that all detected gas resides in it is a quite common value for a PRC Category C objects.

C-22 (= ESO 202-G1): in our present survey no HI line is seen at the optical velocity, $10052\pm 50 \text{ km s}^{-1}$ (LEDA; based on 2 published values), while a tentative line signal is seen at $\sim 9780\pm 30 \text{ km s}^{-1}$, with $W_{50}=220 \text{ km s}^{-1}$ and $I_{HI}=1.4 \text{ Jy km s}^{-1}$. Though no candidates for confusion with our HI spectrum were found within the search area, we cannot be certain that the object was detected, seen the weakness of the tentative line detections and the difference of 272 km s^{-1} (i.e., $5.5\sigma_{V_{opt}}$) between the well-established optical redshift and our HI value. We have therefore marked the spectral line as 'marginal' in Table 2, and we did not derive an HI mass from it.

C-42 (= NGC 4672): it has an elliptical stellar core rotating perpendicularly to the disk and appears to be the end result of the accretion of material in polar orbits in a disk around a pre-existing oblate spheroid, like in the prototype PRC B-19 (Sarzi et al. 2000). The object was detected in the present survey, at $V_{HI}=3202\pm 6 \text{ km s}^{-1}$, as well as previously at Parkes and at Green Bank (see Table 2) at similar velocities, which are all consistent with the mean optical systemic value of $3346\pm 63 \text{ km s}^{-1}$ (LEDA). The integrated line flux of 7.7 Jy km s^{-1} measured at Green Bank (Paper I) is significantly lower than the $12.7\text{-}15.6 \text{ Jy km s}^{-1}$ found at Parkes (Aaronson et al. 1989, and the present paper). No candidates for confusion with our HI spectrum were found within the search area: though NGC 4677, a 13.9 mag object at $10'7$ distance, has a velocity of $3135\pm 40 \text{ km s}^{-1}$ (LEDA), similar to that of the PRC object, it is well outside the telescope's FWHM and classified as SB0 and therefore expected to be gas-poor.

C-48 (= ESO 326-IG6): not detected in the present survey, nor in our Green Bank survey (Paper I), with an almost two times higher rms noise level of 9.5 mJy .

C-52 (= ESO 232-G4): detected in the present survey, at $V_{HI}=4951\pm 20 \text{ km s}^{-1}$. Its published optical systemic velocities are $5083\pm 57 \text{ km s}^{-1}$ (Reshetnikov et al. 2001), based on faint lines, and $5600\pm 200 \text{ km s}^{-1}$ (Fairall 1984), a rather uncertain value. Seen the uncertainties, these values may be consistent with the HI value. Its nuclear spectrum was tentatively classified as LINER: by Reshetnikov et al. (2001). No candidates for confusion with our HI spectrum were found within the search area.

C-53 (= IC 4982): detected in the present survey, at $V_{HI}=6180\pm 16 \text{ km s}^{-1}$. No object is visible on the DSS at

the position given in the PRC, $20^h15^m22^s.4$, $-71^\circ11'13''$ (B1950.0); the galaxy identified as C-53 on Figure 2 in the PRC is actually IC 4982, 1'9 NW of the C-53 position. We therefore used the optical position of IC 4982 as our pointing centre at Parkes and listed its optical characteristics in Table 1. No candidates for confusion with our HI spectrum were found within the search area: IC 4985, 2'4 NE of the target object is a 14.8 mag S0 galaxy at a quite different redshift of $V_{opt}=4442 \text{ km s}^{-1}$ (LEDA), and expected to be gas-poor.

C-55 (= ESO 143-G37): detected in the present survey, at $V_{HI}=3265\pm9 \text{ km s}^{-1}$. The HIPASS data show an HI detection similar to ours. No candidates for confusion with our HI spectrum were found within the search area: no data are available for the small galaxy pair AM2033-620 at 6'2 from the target object.

C-56 (= PGC 128148): detected in the present survey, at $V_{HI}=6873\pm18 \text{ km s}^{-1}$. No candidates for confusion with our HI spectrum were found within the search area.

C-67 (= ESO 75-G55): detected in the present survey, at $V_{HI}=6873\pm18 \text{ km s}^{-1}$. No candidates for confusion with our HI spectrum were found within the search area.

5. Conclusions

Of the 18 PRC objects towards which HI line emission was noted, confusion with one or more galaxies in the telescope beam is suspected, though with varying degrees of probability, in three cases (PRC B-02, B-18 and C-14), while one weak HI line (of PRC C-22) is regarded as a tentative detection only, seen the significant difference between the HI and optical velocities. A previously reported detection of PRC C-14, apparently caused by radio interference, was not reconfirmed. Comparing with literature values as well as HIPASS data, the following eight objects were detected for the first time in HI: PRC B-06, B-19, C-07, C-08, C-53, C-55, C-56 and C-67. Of the 33 observed galaxies 22 now have known radial velocities, five of which were determined here for the following objects with previously unknown redshifts: PRC B-06, C-08, C-53, C-56 and C-67.

Acknowledgements. We are grateful to the ATNF staff at the Parkes observatory and in Epping for their assistance with the observations and data reduction. The Parkes Telescope is part of the Australia Telescope, which is funded by the Commonwealth of Australia for operation as a national facility managed by CSIRO. This research has made use of the NASA/IPAC Extragalactic Database (NED), which is operated by the Jet Propulsion Laboratory, California Institute of Technology, under contract with the National Aeronautics and Space Administration and the Lyon-Meudon Extragalactic Database (LEDA). WvD acknowledges the financial support of the ASTE of INSU for the observations at Parkes.

References

Aaronson, M., Bothun, G. D., Cornell, M. E., et al. 1989, ApJ, 338, 654

Allen, D. A., Norris, R. P., Meadows, V. S., & Roche, P. F. 1991, MNRAS, 248, 528

Arnaboldi, M., Capaccioli, M., Cappellaro, E., et al. 1993a, A&A, 267, 21

Arnaboldi, M., Barbaro, G., Buson, L., et al. 1993b, A&A, 268, 103

Arnaboldi, M., Oosterloo, T. A., Combes, F., Freeman, K. C., & Koribalski, B., 1997, AJ, 113, 585

Bajaja, E., & Martin, M. C. 1985, AJ, 90, 1783

Barnes, L. Staveley-Smith, L., Webster, R. L., & Walsh W. 1997, MNRAS, 288, 307

Boissé, P., Dickey, J. M., Kazès, I., & Bergeron, J. 1988, A&A 191, 193

Brocca, C., Bettoni, D., & Galletta, G. 1997, A&A, 326, 907

Chincarini, G., Tarengi, M., Sol, H., et al. 1984, A&AS, 57, 1

Côté, S., Carignan, C., & Freeman, K. C. 2000, AJ, 120, 3027

Da Costa, L. N., Pellegrini, P. S., Davis, M., et al. 1991, ApJS, 75, 935

Fairall, A.P. 1984, MNRAS, 210, 69

Fairall, A., & Jones, A. 1991, Southern Redshifts Catalogue, Pub. of the Dept. of Astronomy, Univ. of Cape Town, num. 11

Fisher, J. R., & Tully, R. B. 1981, ApJS, 47, 139

Fisher, J. R., Huchra, J. P., Strauss, M. A., et al. 1995, ApJS, 100, 69

Fouqué, P., Bottinelli, L., Durand, N., Gouguenheim L., & Paturel. G., 1990, A&AS, 86, 473

Hawarden, T. G., Longmore, A. J., Goss, W. M., Mebold, U., & Tritton, S. B. 1981, MNRAS, 196, 175

Huchtmeier, W. 1997, A&A, 319, 401 (Paper II)

Keel W. C. 1985, AJ, 90, 2207

Kirhakos, S. D., & Steiner, J. E. 1990, AJ, 99, 1722

Krumm, N., & Salpeter, E. E. 1976, ApJ, 208, L7

Longmore, A. J., Hawarden, T. G., Goss, W. M., Mebold, U., Tritton, S. B. 1982, MNRAS 200, 325

Marlowe, A., Meurer, G., Heckman, T., & Schommer, R. 1997, ApJS, 112, 285

Mathewson, D. S., & Ford, V. L. 1996, ApJS, 107, 97

Reif, K., Mebold, U., Goss, W. M., van Woerden, H., & Siegman, B. 1982, A&AS, 50, 451

Reshetnikov, V. P., & Sotnikova, N. 1997, A&A, 325, 933

Reshetnikov, V. P., Faíndez-Abans, M., & de Oliveira-Abans, M. 2001, MNRAS, 322, 689

Richter, O.-G., Sackett, P. D., & Sparke, L. S. 1994, AJ, 107, 99 (Paper I)

Roberts, M. S., & Haynes, M. P. 1994, ARA&A 32, 115

Sandage, A., & Tammann, R. A. 1981, A Revised Shapley Ames-Catalog of Bright Galaxies, Carnegie Inst. of Washington (RSA)

Sarzi, M., Corsini, E. M., Pizzella, A., et al. 2000, A&A, 360, 439

Skillman, E., Côté, S., & Miller, B. 2002, AJ, in press

Staveley-Smith, L., Wilson, W. E., Bird, T. S., et al. 1996, PASA, 13, 243

van Driel, W., Arnaboldi, M., Combes, F., & Sparke, L. S., 2000, A&A, 141, 385 (Paper III)

van Gorkom, J. H., Schechter, P., & Kristian, J. 1987, ApJ, 314, 457

Whitmore, B. C., Lucas, R. A., McElroy, D. B., et al. 1990, AJ, 100, 1489 (PRC)

Whitmore, B. C. 1991, in: Warped Disks and Inclined Rings around Galaxies, eds. S. Casertano, P. Sackett and F. Briggs (Cambridge University press: Cambridge), p. 60